A C T A G E O P H Y S I C A P O L O N I C A

Vol. 53, No. 1 2005

SEARCH FOR CHAOTIC DYNAMICS MANIFESTATION IN MULTISCALE SEISMICITY

Łukasz KORTAS

Central Mining Institute
Plac Gwarków 1, 40-166 Katowice, Poland
e-mail: l.kortas@gig.katowice.pl

A b s t r a c t

This paper contains a description of the methods of studying non-linear dynamics revealed in the collected data sets, and the estimations of selected parameters of non-linear dynamics. Sets of data referring to seismic phenomena of different origin and, most importantly, different scale of observed rock fracturing and destruction processes were analysed. Collected sets were related to fracturing: starting from a microscale, i.e., seismo-acoustic emission registered in rock samples subjected to compression, through mining induced seismicity, to a macroscale that is represented by earthquakes. The data was examined in terms of the presence of non-linear dynamics and deterministic chaos.

An attempt to quantify the parameters of chaos was made in order to define to what extent the process of cracking and destruction of rocks has features common in different scales. Several parameters of chaotic dynamics were applied.

The fractal dimensions, Lyapunov's exponents, the dimension of reconstructed phase space, and the dimension of the attractor were calculated from descriptors characteristic to seismological processes, i.e., time-space distribution and energy distribution of quakes. The usefulness was assessed of the applied methods of data analysis for the description of seismological processes and seismological hazard evaluation.

Key words: chaos, natural seismicity, mining seismicity, acoustic emission.

1. INTRODUCTION

The examination of every accessible parameter characterising natural and induced seismicity is very important from the point of view of the security of inhabited seismic zones or areas where mining is conducted. It is also an interesting scientific issue. The use of the parameters of non-linear dynamics is one of the ways of describing the development variability of the tremor making processes.

In this paper, different seismic processes are considered as complex dynamic systems that can show certain symptoms of deterministic chaos. To examine and describe chaotic behaviour in physical systems, many concepts and mathematical constructions are used. Here the following will be applied to describe the different-scale seismicity: time series, fractal dimensions, phase spaces and attractors of processes, and Lyapunov's exponents. These concepts will be used to calculate some measures of chaos.

Several authors have conducted similar research in the past. A new element of the studies is an analysis combining different scales and origins of seismic phenomena. Such analysis provides an opportunity to verify the description possibilities and a universal character of the parameters of rock cracking and destruction processes in different conditions, which was the main goal of the work. The minor goal was a qualitative ordering of the possible chaotic behaviour for natural and induced seismicity or seismoacoustic emission based on the calculated estimates. Since the distributions of energy, location and the occurrence of tremors show characteristics of statistic self -affinity, one of the estimates can be a generalised fractal dimension (Idziak and Zuberek, 1995; Marcak, 1995; Mortimer and Lasocki, 1996; Mortimer, 1997; Lasocki and Mortimer, 1998). In the studies of the dynamics of seismic processes it is helpful to make an analysis of their phase spaces and define the estimates of minimal dimensions of spaces and correlation dimension of the attractor (Mendecki, 1997; Radu *et al*., 1997; Mortimer *et al*., 1999a, b; Mortimer, 2000; 2001). The parameters characterising the development of seismic process and sensitivity to disturbance by marginal conditions are also Lyapunov's exponents (Mortimer and Cichy, 2001; Mortimer, 2001).

2. DATA SETS

Data concerning natural seismicity accompanying tectonic tremors and volcanic phenomena were analysed. Tremors generated by the activity of displacement fault of San Andreas in N. and S. California were examined. Three other data sets refer to the Yake-dake volcano in Japan (Volcanism 1, 2) and seismic events near Etna in Sicily.

Next, five sets of data referring to seismicity induced by mining were examined. The first two come from copper mines *Polkowice-Sieroszowice* and *Rudna* in the Legnica–Głogów Copper Mining Area in Poland. They differ as to the region and the time of recorded events. A third data set refers to the tremors caused by mining in one of

the gold mines in S. Africa. The subsequent two sets of events come from the Upper Silesian Coal Basin and are connected with hard coal mining in the *Katowice* and *Wujek* mines.

Apart from that, the author studied six sets of data made as a result of the monitoring of **a**coustic **e**mission (AE) of rock samples from Polish quarries. These sets refer to the uni-axial compression tests (Majewska *et al*., 2000) conducted on 3 lithologically different rocks with dimensions of 31.5×64.3 mm: syenite from Przeborów

Table 1

The characteristics of analysed data sets

No.	Data set		Energy range [J]	Time range
	Area	Number of events		
Natural seismicity				
1	San Andreas, S. California	1422	$2.5\times10^{6} - 7.0\times10^{16}$	4 Jan – 13 Aug ′02
2	San Andreas, N. California	1994	$4.1\times10^{6} - 3.9\times10^{15}$	1 Jan – 15 Aug ′02
3	Yake-dake, Japonia – Volcanism 1	3195	$4.4\times10^{3} - 1.3\times10^{13}$	7 Aug – 24 Aug ′98
4	Yake-dake, Japonia – Volcanism 2	3293	$2.7\times10^{2} - 8.2\times10^{11}$	1 Sep – 31 Dec ′98
5	Etna, Sicily	1506	–	3 Jan ′88 – 26 Dec ′92
Mining induced seismicity				
6	*Polkowice-Sieroszowice* copper mine	1870	$3.2\times10^{3} - 1.0\times10^{9}$	18 Jun ′76 – 31 Jul ′00
7	*Rudna* copper mine	1883	$2.0\times10^{3} - 3.7\times10^{7}$	4 Feb ′84 – 23 Feb ′01
8	Gold mine, RPA	1714	$2.6\times10^{5} - 5.5\times10^{11}$	1 Sep ′90 – 15 Nov ′96
9	*Katowice* hard coal mine	994	$1.0\times10^{2} - 1.0\times10^{6}$	1 Sep ′85 – 04 Sep ′86
10	*Wujek* hard coal mine	507	$5.0\times10^{2} - 6.0\times10^{6}$	20 Nov ′92 – 05 Oct ′95
Acoustic emission / Energy rate				
11	Syenite–P3, stage (b)*)	4795	1–922	$01^{h}19^{m}56^{s}$
12	Syenite–P3, stage (c)	1377	1–2610	$01^{h}05^{m}19^{s}$
13	Granite–S4, stage (a)	2680	1–5654	$00^{h}44^{m}52^{s}$
14	Granite–S4, stage (b)	3701	48–1432	$01^{h}01^{m}40^{s}$
15	Granite–S4, stage (c)	4301	16–2618	$01^{h}11^{m}40^{s}$
16	Sandstone–T13, stage (b/c)	1351	1–3442	$01^{h}19^{m}45^{s}$

*)Compression stages: (a) before destruction, (b) during destruction, (c) after destruction. Explanations to samples P3, S4 and T13 – see Section 2 in the text.

(sample P3), granite from Strzelin (sample S4) and sandstone from Tumlin (sample T13). The spectrum of the generalised fractal dimension $D_q(q)$ and reconstruction of the attractor in the embedded space usually has a different character in different phases and stages of the process of sample destruction (Majewska and Mortimer, 1998; 2000). Therefore, it was necessary to divide the data into appropriate subsets.

In Table 1 detailed information referring to all examined data sets is listed.

3. METHODOLOGY OF FRACTAL ANALYSIS

The analysis started from the verification of multi-fractality of data sets. This was made by calculating generalised fractal dimensions for the distributions of seismicity in the domain of time, distance and energy. Then the phase spaces of the examined phenomena were analysed and the dimension of the attractor for each process was estimated. The last stage of calculations was the estimation of the largest Lyapunov's exponent for the analysed data sets. This parameter is the index verifying the presence of chaotic behaviour in this system.

The analysis of a single sequence of subsequent values of one of the dynamic variables of the system (e.g., energy of subsequent seismic events) can be helpful if the full description of the system is unattainable. They are "time" series timed by the sequence of selected parameters of seismic events registered in time. In this way, the time series of energy, the moment when the tremor occurred, and tremor's location *xy* and *xyz* were determined. The use of a single time series of one variable is a justified generalisation, because such a series is influenced by all other dynamic variables of the examined system (e.g., Packard *et al*., 1980; Takens, 1981; Mane, 1981).

The spectrum of generalised fractal dimension was analysed to examine whether seismic events recorded in individual data sets for the distributions of energy, time and the coordinates of sources represent fractal sets. The generalised fractal dimension was estimated with the use of the generalised correlation sum (Grasberger and Proccacia, 1983). The statistic moment of the order q of the correlation sum is

$$C(R,q) = \frac{1}{N}\sum_{i=1}^{N}\left[\frac{1}{N}\sum_{j\neq i} H\left(R - \left\|x_i - x_j\right\|\right)\right]^{q-1} , \tag{1}$$

where x_i, x_j are any different elements of a data set, N is the number of these elements and $H(y)$ is Heaviside's function taking values: 1 for $y \geq 0$ and 0 for $y < 0$. Heaviside's function adds to the correlation integral only these points that are at a distance shorter or equal to R from the point x_i. If the distribution of a certain physical value has multifractal features, $C(R, q)$ is linearly dependent on R in a bi-logarithmic scale:

$$\log C(R,q) \propto (q-1) D_q \log R , \tag{2}$$

where D_q is an estimate of the generalised dimension.

The D_q value was estimated from the inclination of the curve of eq. (2) both for integer numbers and fractions as well as negative and positive values of parameter q ($q \neq 1$). The inclination was calculated from the selected interval $[R_1, R_2]$ where the relation was linear (Fig. 1). During such calculations, the intervention of an interpreter in choosing an interval of linearity is essential, but it requires the visualization of the results obtained so far.

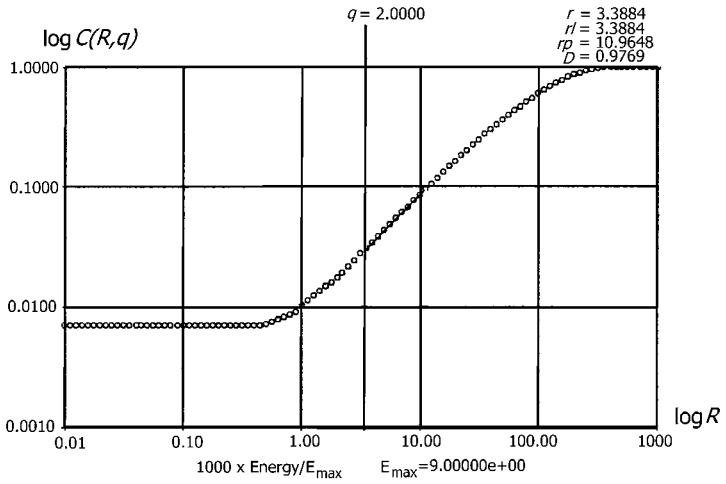

Fig. 1. The dependence of $\log C(R,q)$ on $\log R$ for energy distribution of 1870 tremors recorded in the *Polkowice-Sieroszowice* copper mine, dimension $D_{q=2} = 0.98$.

The phase space of the examined seismological phenomena was investigated in order to get information about the dynamics of seismicity in different scales. Not knowing the form of the equations describing this dynamics, the analysis had to provide data on space dimensions and attractors of the process.

In the study of a dynamic system of multi-dimensional phase space, embedded spaces constructed from time series of individual variables (here: energy, time and location of *xy* epicentres and *xyz* hypocentres) are analysed using Taken's (1981) theorem. The sets of observations of time series $\omega(t)$ of any scalar values are converted into d-dimensional vectors $\mathbf{y}(t)$ with the components being the values of the observations with time delay τ (Baker and Gollub, 1998):

$$\mathbf{y}(t) = \{\omega(t), \omega(t+\tau), \omega(t+2\tau), ..., \omega(t+[d-1]\tau)\} , \tag{3}$$

where $\omega(t)$ is the variable of the system, τ is the time delay.

There are different criterions for choosing the time lag and the minimal embedded phase space dimension optimised for the lowest loss of information in the original

system. Here, following Radu *et al*. (1997) and Mortimer *et al.* (1999b), the time delay is accepted as the first zero of the autocorrelation function.

During the reconstruction of the attractor based on the time series of unknown dynamics, it is necessary that the reconstructed attractor be „embedded" in the space of a sufficient number of dimensions, so that the dynamics of the system is fully represented. So the attractor is reconstructed in a low-dimension space, its "embedded" dimension is calculated and then the Euclidean dimension of the embedded space is increased by 1, the attractor is reconstructed and its dimension in this new space is calculated. This operation is repeated while examining the sequence of embedded spaces of growing dimensions d until the moment of reaching the border value of the dimension of a correlation attractor D_2. Estimations of correlation fractal dimension of the attractor were made by calculating the correlation sum $C(R)$ (Grassberger and Procaccia, 1983) taking $q = 2$ in formula (1). Here x_i, x_j are the points of the attractor, and N is the number of points selected randomly from the whole data set. $C(R)$ gives the average fraction of the points inside a sphere of radius R. The estimation of D_2 in individual d-dimensional embedded spaces was made, similarly to the estimation of generalised fractal dimension. For every variable, the correlation dimension D_2 was calculated for embedded spaces having Euclidean dimensions d ranging from 1 to 15. The results are presented as plots of D_2 *vs.* d. The value of d at the point where the graph is flattened is d_{min} (the smallest embedded dimension) referred to an investigated parameter, i.e., the number of independent variables of the system. Flattening of the curves indicates the presence of coherent structures, which in fact are strange attractors (of fractal dimension) revealing the presence of chaotic behaviour in the system.

The last stage of the analysis was the investigation of the dynamics of phase space through the calculation of the largest Lyapunov's exponent λ_{max}. The largest exponent λ_{max} is the measure of the system trajectory divergence during the evolution. Thus, the speed the system creates or destroys information is the measure of its prediction ability. Negative exponents λ_- have an influence on the process of getting the trajectory closer to the attractor, and positive exponents λ_+ smaller than the maximum positive exponent shorten the time of predictability. To obtain λ_{max}, the divergence of a trajectory close to the selected trajectory is followed. During subsequent estimations of the speed of divergence of two points in time t_n–t_1 evolving from the distance (on their trajectories) L_i to L_{i+1}, it is necessary to choose a new neighbour from time to time (so that the distance between neighbours remains small). Finally, after n repetitions of extending and renormalization of the gap, the largest Lyapunov's exponent is estimated for experimental data based on Wolf's (1985) algorithm with the constant time of evolution (Mortimer and Cichy, 2001). Hence, λ_{max} is given by the formula

$$\lambda_{\max} = \frac{\sum_{i=1}^{n-1} \ln\left(L_{i+1} / L_i\right)}{t_n - t_1} \,. \tag{4}$$

A dynamic system possessing at least one positive Lyapunov's exponent is a chaotic system. The results of the analysis of λ_{max} are presented in the graphs, later in the text. The figures concerning λ_{+} were obtained by selecting different values of the parameters such as: the value of the displacement on the trajectory (*evolv*), fractions of the time between the renormalizations of the gap between the trajectories (*DT*), dimension *dim* of the embedded space or delay *tau*.

4. RESULTS

San Andreas fault

The analysed data set was obtained from the internet database Southern California Earthquake Center. The most complete data (with the depth component) and the newest data available were selected. They come from the catalogue of natural seismicity caused by the activities of the San Andreas displacement fault in California in 2002.

Analysing annual activities of the fault over the last several decades, the concentration of tremors in two areas was found. The first is located in N. California in the region between the cities of Mojave and Bakersfield and expands NE from these cities. The second area is situated in S. California, east of the city of San Diego, near the border with Mexico and from there it expands NW. The whole data set was divided into two subsets: the first included the events registered between 32º and 34º and the second, between 35º and 37º N. Subsets were called S. and N. California, respectively. The coordinates were converted from a polar system into rectangular one and the distances were expressed in kilometres. The results are shown in Fig. 2.

The most heterogeneous is the data set for energy and location *xyz*. The distributions of coordinates *xy* and time also show certain heterogeneity, and the distribution of coordinates *xy* is similar to that of coordinates *xyz*. The shape of the spectra for dis-

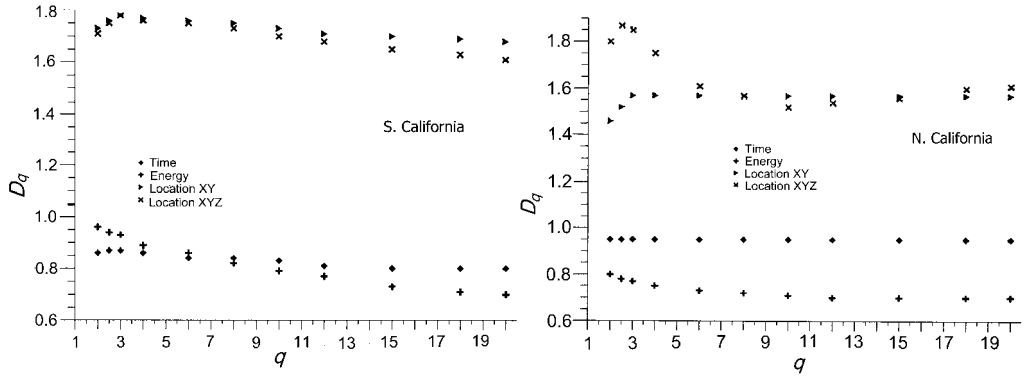

Fig. 2. Curve $D_q(q)$ for the distributions of time, energy, coordinates *xy* and *xyz* of 1422 tremors recorded in S. California and 1994 tremors in N. California in January–August 2002.

tributions of *xy* and *xyz* evidences a small influence of coordinate *z* which is caused by the fact that more than 3/4 of the registrations of tremors in this data set come from the depth 6–7 km and the rest is ranging 0.1–15 km (single tremors achieve a maximum depth of 36.1 km). Such a discrepancy does not occur in the N. California set where the depths of the tremors are uniformly distributed in the interval of about 0.1–12 km (max. 44.6 km).

In N. California (Fig. 2), the most heterogeneous is the data set of hypocentre coordinates *xyz*. The distribution of coordinates *xy* also shows certain heterogeneity. The scale of heterogeneity of the distributions of time of tremors is very small and D_q concentrates near unity. The shape of the distribution and value of generalised dimension for energy ($D_\infty = 0.7$) is very similar to the respective distribution for the S. California. Apart from that, similar patterns in both data sets from San Andreas Fault region are found in distributions of the time of tremor occurrence.

In Fig. 3 the analysis of phase spaces of seismicity in S. and N. California is presented. The values of dimension D_2 of subsequent reconstructed attractors of phase space grow with growing dimension *d* of Euclidean space reaching more or less distinct saturation for different values of *d*. In the case of energy, the analysed curves are very similar. Levels of saturation for both data sets were not observed. The saturation may occur for S. California only for $d > 15$ (the change in curve inclination is visible),

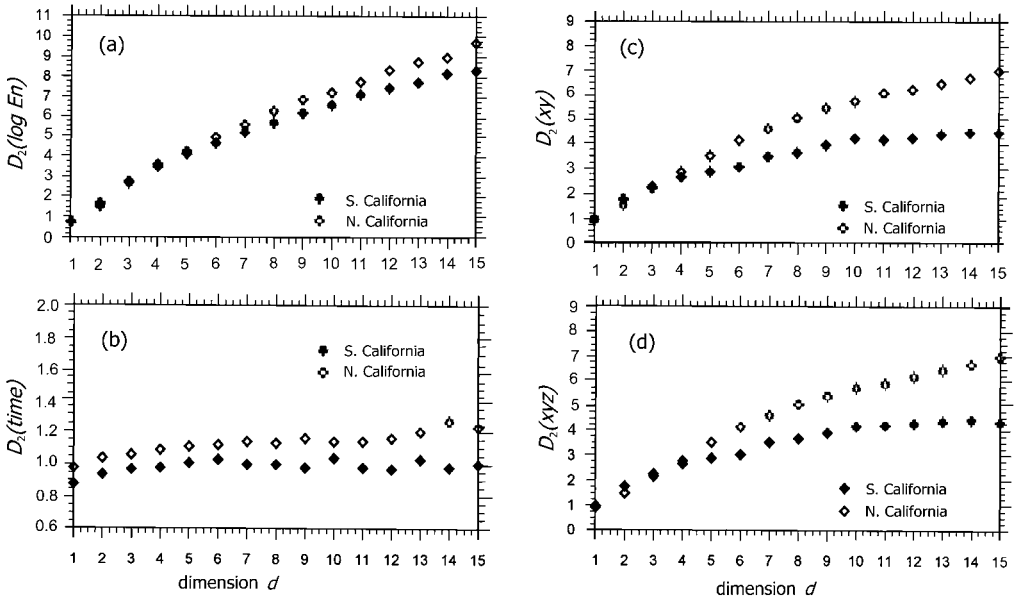

Fig. 3. Correlation dimensions D_2 of the attractors *vs*. dimension *d* of Euclidean spaces embedded in the phase space of tremors recorded in S. and N. California in January–August 2002: (a) energy log, (b) time, (c) distance *xy*, and (d) distance *xyz*.

while for N. California there are no such circumstances. For the time distribution, the curves differ from each other, although the shape of both curves is similar. The saturation level for S. California starts from $d > 3$ and for N. California from 4. The value of dimension D_2 of the attractor in the first case is almost one, while in the other case it oscillates around 1.15. The saturation level is, however, more stable for the data of N. California than for the second set, which can be caused by higher regularity of tremors in this area. Such a distinction is also observed in the multi-fractal spectra ($D_\infty = 0.89$ and 0.90, respectively). The curves of distance *xy* and *xyz* for both data sets referring to the seismicity of California are almost identical, which indicates again a small impact of the component *z* on the result (hypocentres of Californian earthquakes are situated shallowly and approximately at the same depth). In S. California, distinct saturation appears from $d = 10$ for both *xy* and *xyz* distributions. The dimension of the attractor in both cases is about 4.3. For the second data set, the saturation is not

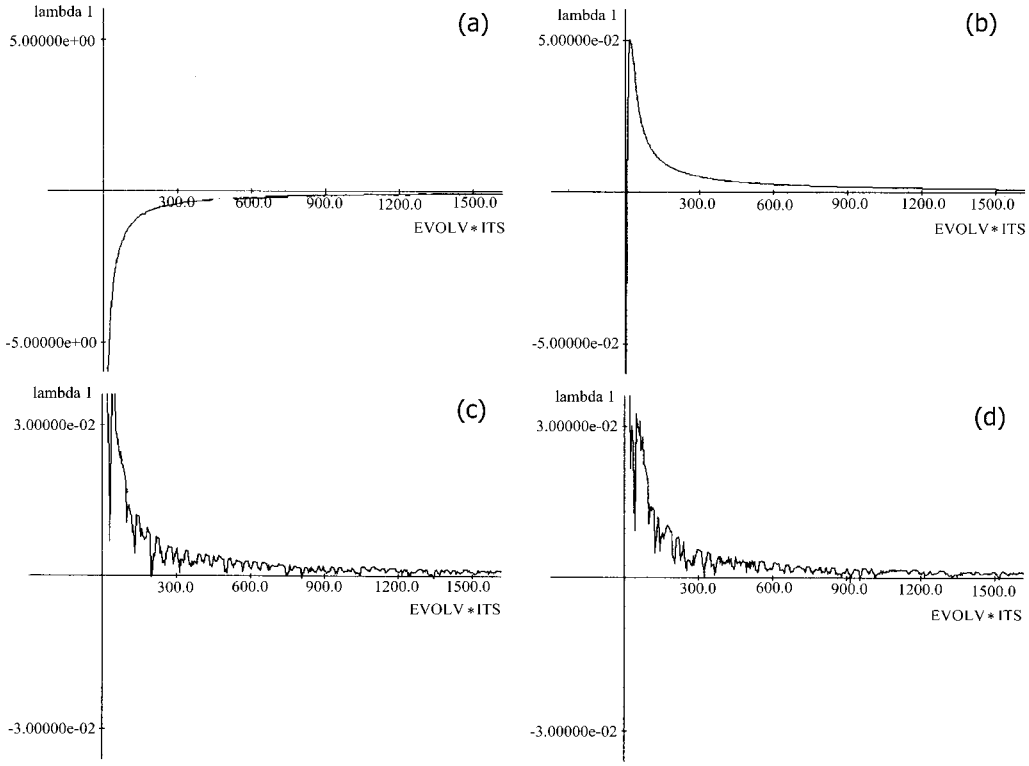

Fig. 4. Values of λ_{max} for tremors recorded in S. and N. California in January–August 2002: (a) energy log, (b) time, (c) distance *xy*, (d) distance *xyz*. Dim = 8, tau = 4, evolv = 4, dt = 1, scalmx = 100, scalmn = 10.

observed so it is not possible to determine the dimensions of the attractor. This is true for both surface and space distributions of the event sources. This is probably connected with the dissimilarity of the tremor occurrence mechanism in the northern part of the region. The saturation in these cases and in the energy case may occur for $d > 15$.

The estimated largest Lyapunov's exponents for S. and N. California are presented in Fig. 4. The analyses made separately for both regions produced very similar results. Positive values of λ_{max} were obtained, confirming the presence of deterministic chaos for the distributions of all the parameters except for energy. The curves for surface and space distributions in both regions show clear similarity.

The volcanoes of Yake-dake and Etna

The data from the catalogue of natural seismicity caused by volcanic activity of Yake-dake volcano on Honshu in Japan (Lasocki and Kustowski; 2002) and Etna in Sicily were analysed similarly to the records from California.

Yake-dake, like other Japanese volcanoes, is part of five "volcanic arches". These arches meet on a triple junction on the island of Honshu, very close to Yake-dake. This volcano belongs to the NE arch of Honshu, which, together with the Kuryl arch is NE directed. Both arches are formed as a result of the subduction of the Pacific Plate under the Eurasian Plate. Volcanoes inside these arches form the NW part of the Pacific "Ring of Fire".

The catalogue includes over 7 thousand events (0.1–5 M); about half of them were recorded within one month of 1998, while the rest are the tremors recorded during several consecutive months of the same year. Therefore, the set was divided into two smaller subsets: Volcanism 1 and Volcanism 2. In Fig. 5 the results of the $D_q(q)$ analysis for the distributions of logarithm of energy of events, and surface and time of tremors are presented.

Etna is situated on the east coast of the island Sicily, Italy. This is a shield volcano, but its summit, consisting of many joint craters, cracks and inlets is regarded as a stratovolcano. Etna is supported by four main shallow volcanic focal points. The set of natural seismicity data, generated by the volcanic activities of Etna is the only set analysed here that does not contain information on the energy of tremors. Therefore, only space-time distribution of 1506 recorded events was examined.

During the analysis of spectra of generalised dimension (Fig. 6), considerable discrepancies in the shape of curves for all the examined parameters were observed. The distributions of time, *xy* and *xyz* show a rather high heterogeneity and do not concentrate near one value of dimension.

Phase spaces analysis for seismicity of the discussed regions was made. Time series of variables recorded in two subsequent time intervals (Volcanisms 1 and 2) were analysed. Because the data on the energy of recorded tremors are not complete for

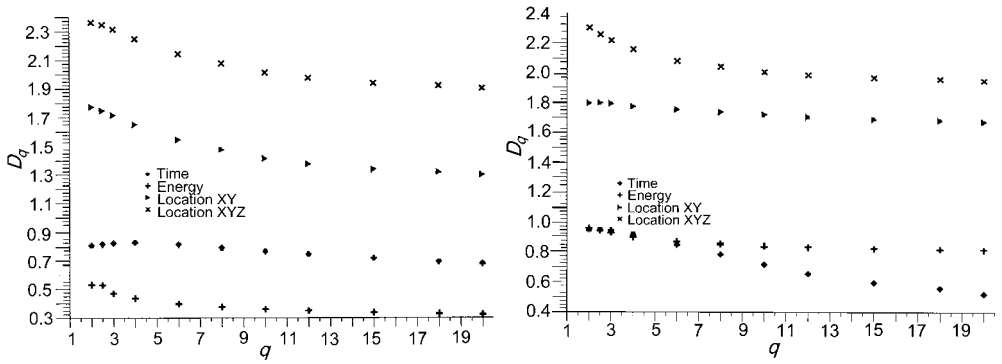

Fig. 5. Curves $D_q(q)$ for the distributions of time, energy and source coordinates *xy* and *xyz* of 3199 tremors recorded in the region of volcanic activities in Japan in August 1998 (left), and 3293 tremors recorded between September and December 1998 (right).

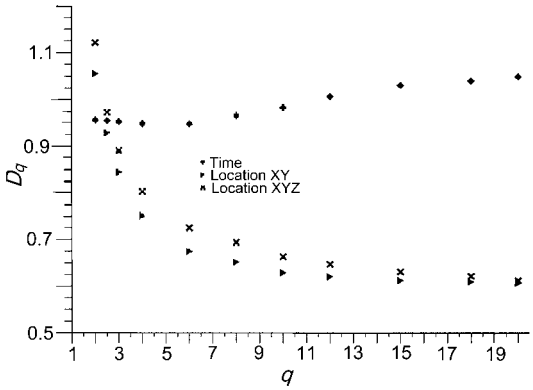

Fig. 6. Curves $D_q(q)$ for the distributions of time, source coordinates *xy* and *xyz* of 1506 tremors recorded in the seismically active region in Sicily from January 1988 to December 1992.

Etna, the reconstruction of the phase space of seismicity in that region was made using time series of 3 variables (for results see Table 3).

Copper mines

The copper deposit of the Legnica-Głogów Copper Mining Area consists of one seam of copper-carrying shale, up to 1 m thick, situated below ore-surrounded sandstones and overlying ore-surrounded dolomites. The deposit is exploited using the chamber -pillar method of shooting at a depth of about 1100 m below ground level. The seismicity of the area of exploitation is one order of scale stronger than that of the Upper Silesian Coal Basin mines (Laskownicka, 1999). The data from the region G-23 being

a part of the division PW of *Polkowice-Sieroszowice* (1870 events) and records from the joint regions G-12 of the division PG and G-14 in the division PZ of *Rudna* (1883 events) were chosen for analysis. Since the data referring to the depth of the tremors are incomplete and carry the biggest errors, only energies, times and coordinates of the tremor epicentres were used in the analysis. The results concerning generalised dimensions D_q are presented in Fig. 7.

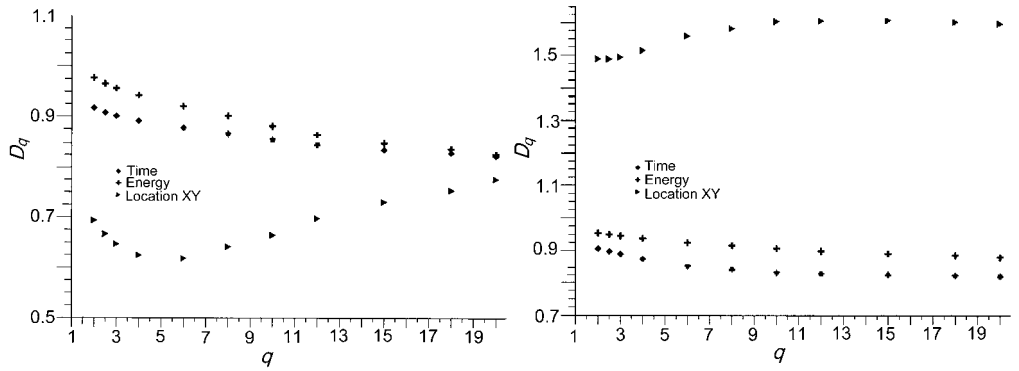

Fig. 7. Curves $D_q(q)$ for the distributions of time, energy and coordinates of the epicentres of 1870 tremors recorded in *Polkowice-Sieroszowice* mine for June 1976 – July 2000 and 1883 tremors in *Rudna* mine for February 1984 – February 2001.

The analysed distributions have multifractal features, but they represent sets of different heterogeneity. For the distribution of coordinates *xy* the scale of heterogeneity is larger than for the distribution of time and energy. Moreover, in case of *xy*, the generalised dimension is growing up for $q > 6$. This effect can be caused by the growth of the error in the determination of estimate of D_q for large values of parameter q. For low q, the interval of the linearity of relation (2) in the central part of the curve is much more distinct and created by more points than for the high values of this parameter, especially with a relatively short series of data. For bigger q, the linear part of the curve becomes shorter and most points are grouped in the initial and final part of the curve (depopulation and saturation). This can cause "over-estimation" of dimension D_q. Such situation reoccurs in several other charts (also for Etna, as well as *Rudna* and *Wujek* mines). However, usually such "over-estimation" of the dimension does not exceed 0.10.

Going back to the analysis, one can conclude that multifractal spectra $D_q(q)$ for time and energy are very similar for both study regions, which seems fully justified due to very similar ways of exploitation. The spectra of the distributions of coordinates are different, which is probably related to different geomechanical conditions in this region of the mine. Table 3 contains the results of the phase space and λ_{max} analysis.

Gold mine in South Africa

The gold deposits in S. Africa make dense networks of small ore-bearing stock works in metamorphic strata. The area of the occurrence of the deposit, Witwatersrand Basin, is disturbed by numerous faults and dykes. The exploitation is run in the wall system with the front width of about 30 m, to a depth of 3000 m below ground level. The events of similar form of occurrence and distribution as the high-energy tremors in Polish hard coal mines are characterised by energies about one order stronger (Laskownicka, 1999). The studies were carried out on the data set originally registered in one of the gold mines of S. Africa. The catalogue includes 1714 tremors.

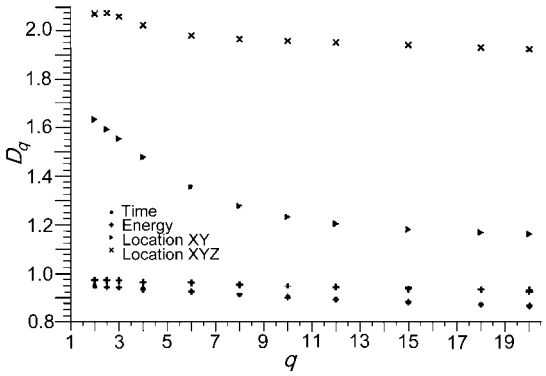

Fig. 8. Curves $D_q(q)$ for the distributions of time, energy, source coordinates *xy* and *xyz* of 1714 tremors recorded in a gold mine in S. Africa from September 1990 to November 1996.

The spectra $D_q(q)$ (Fig. 8) for time and energy are in this case very similar. The curves indicate low heterogeneity of the data set and concentrate near 0.9–1.1. Fractal dimensions close to the Euclidean dimension (here: 1) of the examined value may indicate a random character of data in the set. The graphs of the distributions of coordinates *xy* and *xyz* have much higher inclination than the other ones. This indicates that these data sets are more heterogeneous.

Hard coal mines in Poland

The deposits of hard coal in the *Wujek* and *Katowice* mines (neighbouring on the north) are situated in the central part of the Upper Silesian Coal Basin, in the southern slope of the main saddle. In the south, the border is made by the Kłodnicki fault that throws layers towards the main trough. In the mining areas down to a depth of 1000 m there occur the Quaternary and Upper Carboniferous formations. *Wujek* and *Katowice* are ones of the most seismically endangered mines of the Upper Silesian Coal Basin with the third degree of bounce hazard. The examined eastern region is limited from the south and east by the faults of big throws and from the north by the workings of the upper level.

The first data set contains 994 tremors from one year observation of seismicity induced by the exploitation of longwall 532 in *Katowice*. The system of coordinates was connected with the centre of the exploited wall. The other data set refers to 507 tremors generated during the exploitation in *Wujek* on longwall 33, level 501, at a depth of 600-680 m. This level was wholly exploited by wall system into two main layers with the wall collapse. It consists of the series of sandstone and ooze shale reaching a thickness of several to several tens meters (average 45 m). The whole exploitation was accompanied by high seismicity and the rock mass should be regarded as disturbed and unstable.

Curves $D_q(q)$ for time obtained for *Katowice* were very similar to multifractal spectra for the gold mine (Fig. 9). This distribution also indicates very low heterogeneity of the data set and concentrates in the range 0.95–1.05. The distributions for coordinates *xy* and *xyz* are more heterogeneous than the other ones.

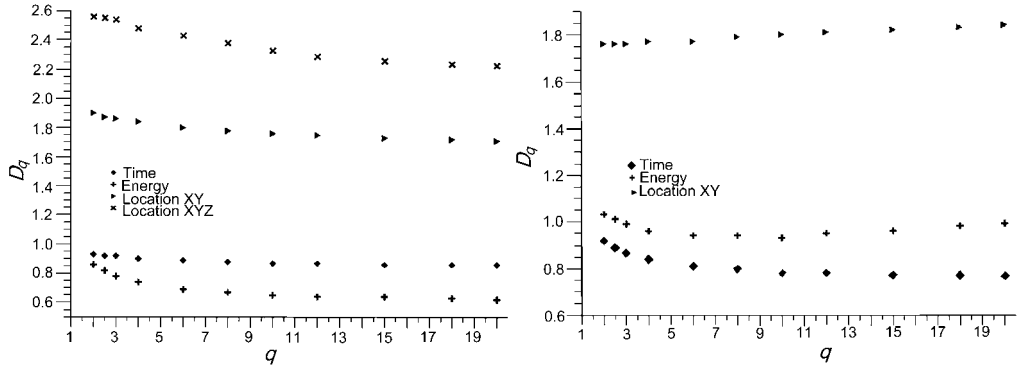

Fig. 9. Curves $D_q(q)$ for the distributions of time, energy, source coordinates *xy* and *xyz* of 994 tremors recorded in *Katowice* from September 1985 to September 1986 and 507 tremors in *Wujek* from November 1992 to October 1995.

For *Wujek*, slightly different results were obtained. The spectra (Fig. 9) are of multifractal character and represent sets of different heterogeneity. For the distribution of coordinates *xy* and time of occurrence, the heterogeneity scale is larger than for energy distribution.

The results of the analysis of phase space of the seismicity of *Katowice* and *Wujek* are listed in Table 3. Because of the incompleteness of the records of depth component in the data set of *Wujek*, the reconstruction of the attractor from the time series of hypocentres coordinates was not made.

Acoustic emission in rock samples

Acoustic emission was recorded during the uni-axial compression tests of rock samples performed in a cylindrical press, with the constant speed of circumferential de-

formation (10^{-5} to 10^{-6} m/s). An *AE* detector was applied. Recorded seismo-acoustic signals were transferred into a pre-amplifier of the load and then into a digital *AE* analyser connected to a computer. With a special software it was possible to analyse the following parameters: acoustic activity, intensity of released energy (energy rate), mean energy of signals and frequency spectrum of selected signals, as well as to record the actual time of emission of a particular seismo-acoustic signal in seconds.

The compression test was divided into the following stages: (a) before, (b) during and (c) after destruction of the sample. For sample **P3** of **syenite from Przeborów** stages (b) and (c), with 4795 and 1377 records, respectively, were distinguished. Stage (a) for sample P3 was neglected, because this subset contained only 540 records and was not representative for the stage before the destruction. For sample **S4** of **granite from Strzelin** all three stages were observed with the following number of records: (a) 2680, (b) 3701 and (c) 4301. For sample **T13** of **sandstone from Tumlin** we recognised stages (b) or (b) and (c), and they were analysed as a whole.

The energy rate distribution of seismo-acoustic impulses is shown in Fig. 10. The *AE* energy distribution in sample P3 has a multifractal character. Small inclination of the curve indicates homogeneity of the data set. Spectrum $D_q(q)$ changes when the test enters phase (c). High inclination of the curve for q from the interval 2–4 indicates strong heterogeneity of the data set. The spectra $D_q(q)$ for the intensity of energy emitted during the compression of sample S4 are very similar in all three phases of the destruction process. These distributions show low heterogeneity and concentrate near the value of 0.9–1.0.

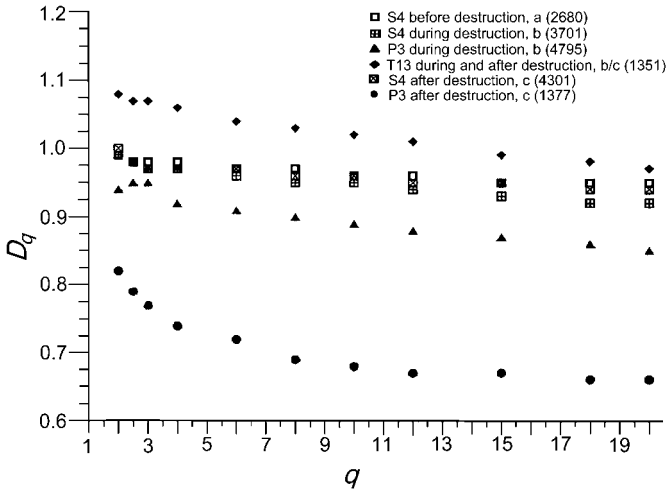

Fig. 10. Spectra $D_q(q)$ for the distribution of the intensity of *AE* impulses energy recorded in different stages of the compression test of samples: S4 (granite), P3 (syenite) and T13 (sandstone).

For sample T13 it was observed that the spectrum shape is close to that of P3 during the destruction. The values of generalised dimension are, however, noticeably higher for T13 and grow the highest among all the analysed samples and stages of acoustic emission. At the same time, they are the closest to one, which can indicate random distribution of the intensity of energy emitted at the same stage of the test.

The attractor in phase space of *AE* was reconstructed based on time series of the intensity of energy in the above-mentioned stages of the compression test (Fig. 11). In stage (c) for P3 the level of stabilization D_2 is clear and occurs from $d = 7$. The dimension of the attractor for this part of the sample destruction process is 3.41. In stage (b) the reconstruction of the attractor is impossible. Curve D_2 for d reaches 8.28 for $d = 15$. For S4 in stage (a) the level of saturation occurs for $d = 11$ and the dimension of the attractor can be defined as 4.42. In stage (b) the saturation is less clear and the saturation interval starts further from $d = 12$. Dimension of the attractor is 5.74. In stage (c) a saturation interval is not observed for $d = 1$–15, which could be a confirmation of the random distribution of data in this set.

The values of dimension D_2 of the attractor, reconstructed from the time series of *AE* energy intensity, in sample T13 reach the saturation level for $d = 8$–10. The dimension of the attractor is 3.59. The values of the dimension still grow and for $d > 12$, a second interval of saturation can be noticed. The existence of this interval is probably connected with strong "noise" in the data at the last stage of the test and is not

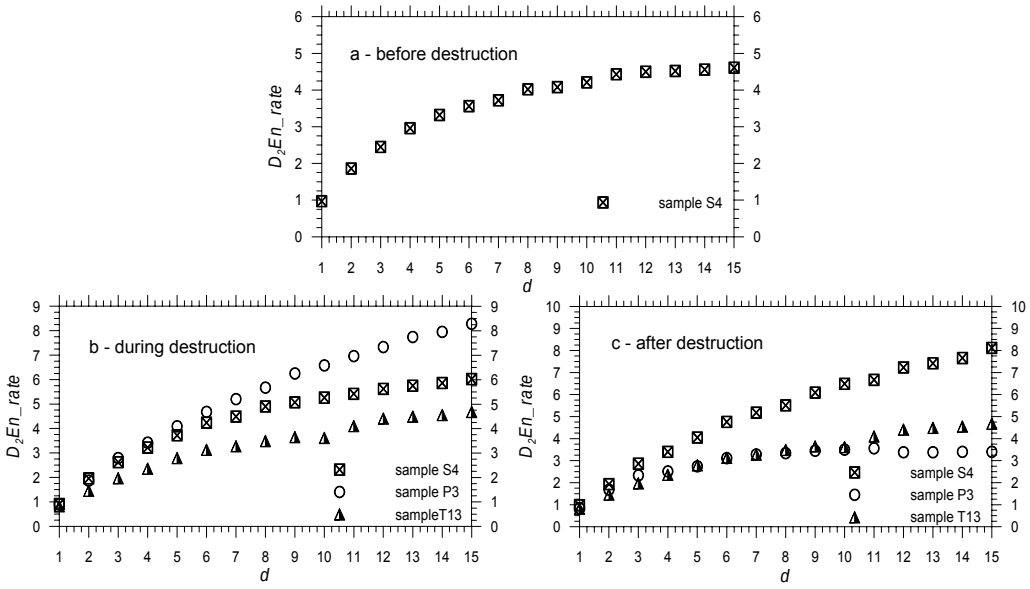

Fig. 11. Correlation dimensions D_2 of the attractors depending on the dimension of Euclidean spaces embedded in phase space for energy rate of *AE* recorded in the compression test of samples: S4 –in stages (a), (b), (c) within $1^h11^m40^s$, P3 – in stages (b) and (c) within $1^h05^m19^s$ and T13 during and after the destruction within $1^h19^m45^s$.

taken into account during the interpretation. Moreover, the shape of curve $D_2(d)$ for $d = 1–10$ is almost identical with that for sample P3. For the results of the largest Lyapunov's exponent estimation, see Table 3.

5. INTERPRETATION

The assessment of the analysed multi-scale seismicity cases consists of an attempt to find certain general rules and not to make the only possible determination of the definite values of parameters. Numerical values of the estimates allow only a qualitative systematisation of the observed chaotic behaviour in the field of induced and natural seismicity, and seismoacoustic emission. The results were grouped into certain sets. The collected numerical values do not have a character of evidence on the presence or absence of chaos, but they do show the problems and the direction of further research.

Errors made during the determination of fractal dimensions can have different origins. Estimation of dimensions may be influenced by the method of its determination, finite number of events in data sets, the size of analysed samples, limited area of analysed space, as well as the accuracy of localizing seismic events. The value of generalised fractal dimensions depends on the choice of a linear part of the curve made by the interpreter. There are no objective criteria, so it is easy to introduce error related to the subjective choice of scale R. The interval of the values of R from which the estimate of generalised dimension is determined, usually changes with changing parameter q. It is recommended to use the same intervals of linearity of function $\log C(R,q)$, so that comparable results of temporal variability of fractal dimensions for different q can be achieved.

On the curve $\log C(R,q)$ *vs.* $\log R$, the so-called depopulation and saturation effects (Nerenberg and Essex, 1990) are observed. The first is connected with the fact that in the initial phase of calculations there are too few data and they are indistinguishable, so the initial points of the graph flatten the curve. The other, occurring at the end of the graph and manifesting itself by the growing density of points on one level, is caused by the close vicinity of the end of the set, and consequently by the fact that D_q takes the same value in last iterations. Depopulation and saturation can significantly influence the linear fragment of the curve whose inclination enables the reading of the value of a fractal dimension. This influence is the greater, the shorter is the examined data set (De Luca *et al*., 1999).

The accuracy of localizing seismic events depends on several factors, such as the spatial configuration of the seismic network, the accuracy of reading the arrival times of the seismic wave, as well as the speed models assumed. The dispersion of errors made in this way can be important for the results. Because of this, and also because of the errors introduced by a wrong choice of R interval, it is more important to get the correct character of dimension changes with changing parameter q than to have the exact value of dimensions.

At the present stage of studies, the inclination changes of the graph of dimensions of reconstructed attractors or the absence of stabilization level have not been documented yet and they are possibly related to growing noise levels or the so-called false neighbours when Euclidean dimension is too low compared to the dimension of space (Majewska and Mortimer, 2000).

In Table 2, the calculated estimates of fractal dimensions D_2 and D_∞ (estimated by $D_{q=20}$) for all the data sets and distributions of the examined quantities are listed.

In Table 3, the dimensions of phase spaces for the analysed data sets are presented together with the estimates of the attractors' dimensions. Sign > means the lack of a clear level of stabilization of the curve, which probably entails a greater number of dimensions of the reconstructed phase space and bigger dimension of the attractor. Sign >> was attributed to the results of the phase space examination when we have no such premises. This suggests a much larger number of dimensions of the reconstructed phase space and a larger dimension of the attractor.

Table 4 shows the results of the analysis of the largest positive Lyapunov's exponents: the signs of λ_+ for subsequent values distributions. Sign +/– refers to the systems where λ_+ oscillated between + and – on the whole length or in the final part of the curve.

Based on the results of the **generalised dimension** spectra analysis, partially collected in Table 2, it can be stated that the distributions of the parameters of the analysed seismic phenomena have a fractal structure.

For the distributions of coordinates, times of occurrence and energy of tremors accompanying the cracking processes and manifesting themselves as tremors in mines, tectonic tremors or *AE*, the linearity of relation (1) was obtained, confirming a multifractal character of the examined data sets.

Multifractal spectra $D_q(q)$, defined for tremors **energy** can be divided into two main groups. The first one includes only four spectra relating to the *Katowice* mine, N. and S. California and *AE* for the syenite sample in the stage after destruction (P3c). The curves in this group suggest strong multifractality and the values of dimension D_∞ are approximately 0.62–0.7, which proves self-similarity of the energy distribution. The second group includes spectra for the remaining data sets: Volcanism 2, copper and gold mines, the *Wujek* coal mine, *AE* for the samples of granite, sandstone and syenite in stage (b). Energy distributions of *AE* are referred to the intensity of energy and not to the energy of a single impulse. In this group the curves showed slightly weaker heterogeneity and values of D_q are changing within the range of 0.82–0.99. High values of D_∞ in comparison to D_2 (increasing curve slope) in a few cases may be linked to the D_q calculation error. Spectra $D_q(q)$ defined for energy of tremors recorded in the area of the volcano Yake-dake in the first period cannot be included in any of the groups mentioned above. The spectrum for the subset Volcanism 1 indicates strong multifractality. Very low values of the dimension indicate strong self-sim-

Table 2

Fractal dimensions D_2 and D_∞ for all data sets and all parameters studied

No.	Area	Number of events	Energy		Time		*xy*		*xyz*	
			D_2	D_∞	D_2	D_∞	D_2	D_∞	D_2	D_∞
Natural seismicity										
1	San Andreas, S. California	1422	0.96	0.70	0.86	0.80	1.73	1.68	1.71	1.61
2	San Andreas, N. California	1994	0.80	0.70	0.95	0.95	1.46	1.57	1.80	1.61
3	Yake-dake, Japan – Volcanism 1	3195	0.57	0.38	0.81	0.68	1.77	1.30	2.36	1.90
4	Yake-dake, Japan – Volcanism 2	3293	0.97	0.82	0.95	0.52	1.80	1.67	2.30	1.95
5	Etna, Sicily	1506	–	–	0.96	1.05	1.06	0.60	1.12	0.61
Mining induced seismicity										
6	*Polkowice-Sieroszowice* copper mine	1870	0.98	0.82	0.92	0.82	0.69	0.77	–	–
7	*Rudna* copper mine	1883	0.95	0.88	0.91	0.82	1.50	1.60	–	–
8	Gold mine, RSA	1714	0.97	0.93	0.95	0.87	1.63	1.16	2.07	1.92
9	*Katowice* coal mine	994	0.86	0.62	0.93	0.85	1.90	1.71	2.56	2.23
10	*Wujek* coal mine	507	1.03	0.99	0.92	0.77	1.76	1.84	–	–
Acoustic emission										
11	Syenite–P3, stage (b)	4795	0.94	0.85	–	–	–	–	–	–
12	Syenite–P3, stage (c)	1377	0.82	0.66	–	–	–	–	–	–
13	Granite–S4, stage (a)	2680	0.99	0.95	–	–	–	–	–	–
14	Granite–S4, stage (b)	3701	0.99	0.92	–	–	–	–	–	–
15	Granite–S4, stage (c)	4301	1.00	0.94	–	–	–	–	–	–
16	Sandstone–T13, stage (b/c)	1351	1.08	0.97	–	–	–	–	–	–

ilarity of events and non-random distribution of the energy. This fact clearly distinguishes that seismicity type from Volcanism 2 and the rest of studied phenomena.

Spectra $D_q(q)$ defined for the **time** of the occurrence of tremor, in six out of ten cases stabilize between the values of dimension 0.77 and 0.87. These include: spectra referring to time distributions of the tremors induced by coal, copper and gold mining and caused by the activity of San Andreas fault in S. California. A separate group consists of the spectra obtained for the distributions of times of the tremors caused by the

Table 3

Estimation of phase space dimensions d_{min} and the dimension of the reconstructed attractor D_2

No.	Area	Number of events	Energy		Time		*xy*		*xyz*	
			d_{min}	D_2	d_{min}	D_2	d_{min}	D_2	d_{min}	D_2
Natural seismicity										
1	San Andreas, S. California	1422	>15	>8.32	3	1.00	10	4.32	10	4.29
2	San Andreas, N. California	1994	>>15	>>9.69	4	1.16	>15	>7.01	>15	>7.00
3	Yake-dake, Japan – Volcanism 1	3195	10	6.89	3	1.09	11	5.34	13	6.18
4	Yake-dake, Japan – Volcanism 2	3293	>>15	>>9.81	4	1.08	7	4.25	6	4.13
5	Etna, Sicily	1506	–	–	6	1.18	>15	>7.11	10	4.14
Mining induced seismicity										
6	*Polkowice-Sieroszowice* copper mine	1870	>15	>8.35	4	1.11	>15	>8.29	–	–
7	*Rudna* copper mine	1883	>15	>8.37	4	1.10	>15	>8.15	–	–
8	Gold mine, RSA	1714	>15	>8.71	8	1.30	>15	>9.23	>15	>9.27
9	*Katowice* coal mine	994	>15	>8.13	5	1.14	14	7.92	13	6.83
10	*Wujek* coal mine	507	13	6.49	5	1.12	11	5.74	–	–
Acoustic emission										
11	Syenite–P3, stage (b)*	4795	>15	>8.28	–	–	–	–	–	–
12	Syenite–P3, stage (c)	1377	7	3.41	–	–	–	–	–	–
13	Granite–S4, stage (a)	2680	11	4.42	–	–	–	–	–	–
14	Granite–S4, stage (b)	3701	12	5.81	–	–	–	–	–	–
15	Granite–S4, stage (c)	4301	>15	>8.12	–	–	–	–	–	–
16	Sandstone–T13, stage (b/c)	1351	8	3.59	–	–	–	–	–	–

*) Compression stages: (a) before destruction, (b) during destruction, (c) after destruction. Explanations to samples P3, S4 and T13 – see Section 2 in the text. Symbols > and >> are also explained in the text.

Yake-dake volcano in Japan. Their strong heterogeneity combined with low values of D_∞ points to a different tremor-making process than the one occurring in mining and the activities of the San Andreas fault. Weaker self-affinity and similar, almost mono-fractal behaviour characterises spectra $D_q(q)$ for *Polkowice-Sieroszowice*, *Rudna*, *Katowice* and the gold mine in S. Africa. A particularly good repeatability of results was obtained in the case of copper mines. The highest value of D_q was achieved by spectra for tremors in the area of Etna (increasing curve slope, probably affected by a calcula-

Table 4

Largest Lyapunov exponents λ_{max} for all data sets and parameter distributions

No.	Area	Number of events	Energy sign of λ_{max}	Time sign of λ_{max}	*xy* sign of λ_{max}	*xyz* sign of λ_{max}
Natural seismicity						
1	San Andreas, S. California	1422	–	+	+	+
2	San Andreas, N. California	1994	–	+	+	+
3	Yake-dake, Japan – Volcanism 1	3195	–	+	–	–
4	Yake-dake, Japan – Volcanism 2	3293	–	+	+	+
5	Etna, Sicily	1506		+	–	+
Mining induced seismicity						
6	*Polkowice-Sieroszowice* copper mine	1870	–	+	–	
7	*Rudna* copper mine	1883	+/–	+	+	
8	Gold mine, RSA	1714	–	+	+/–	+/–
9	*Katowice* coal mine	994	+/–	+	+/–	+/–
10	*Wujek* coal mine	507	–	–	+/–	
Acoustic emission						
11	Syenite–P3, stage (b)	4795	+			
12	Syenite–P3, stage (c)	1377	+/–			
13	Granite–S4, stage (a)	2680	+			
14	Granite–S4, stage (b)	3701	+			
15	Granite–S4, stage (c)	4301	–			
16	Sandstone–T13, stage (b/c)	1351	+/–			

tions error) and in N. California, whose D_∞ = 1.05 and 0.95 indicate poor self-similarity of events. The curves indicate a high heterogeneity of distribution for Etna and high homogeneity for N. California.

The multifractal spectra for the distributions of the **epicentres** of tremors in most of the examined cases group around D_∞ = 1.54–1.84. These spectra show a rather weak multifractality and the value of dimension shows smaller self-affinity of events. The value of 1.84 for *Wujek* suggests that the epicentre distribution is closer to random than in the other cases. The other spectra show strong multifractality obtained using data of *Polkowice-Sieroszowice* and Sicily (D_∞ = 0.6, 0.77) as well as S. Africa, and

Volcanism 1 of Japan (D_∞ = 1.16–1.3). The latter spectra also indicate greater self-similarity within data sets.

As to the distribution of **hypocentres**, the lack of influence of the component *z* on the result is visible in the data from S. California and the area of Etna. For N. California this influence is present but is very insignificant. This is caused by the fact that the hypocentres of Californian earthquakes are situated shallowly and approximately at the same depth. The focal points of the tremors around Etna in most cases (89%) occur at a depth of 0-50 m. The values of dimensions in these cases confirm that the vertical size of these sets is small compared to their horizontal size. For the data concerning volcanism in Japan and gold mining in S. Africa, a clear change of the shape of the spectra and D_∞ of generalised dimensions for the distribution of hypocentres was observed compared to the surface distribution of the focal points of tremors. These spectra for Volcanisms 1 and 2 are very similar; they are multifractal and point to data self-similarity. A similar situation exists for the hypocentres of tremors in the *Katowice* mine, although values of D_∞ are higher than in the other cases.

The studies on the **phase space** of the seismicity of different scale was supposed to provide data on their dimensions, i.e., on the number of independent variables describing the process and on its attractors. This has a significant consequence for the dynamics of the analysed processes.

According to Takens's (1981) theorem, in order to reconstruct the phase space from the time series, any variable can be used, because such a series is influenced by all other dynamic variables of this system. In this work, phase spaces were reconstructed from time series of different variables and one could expect that they will describe the analysed seismic processes in the same way. It is, however, not the case, because different results were obtained for time series of energy than for time and tremor sources distributions. Similar results refer to the reconstruction of the space from sequences *xy* and *xyz*. Such a situation can be related to, e.g., the accuracy of the determination of individual variables, cutting off some parts of data by the assumed energy thresholds and consequently the existence of "false neighbours" or the influence of other factors, e.g., in the seismicity induced by the change of the progress of the longwall (time distribution fluctuations). Similar results, different d_{min} for different variables, were obtained by, e.g., Mendecki and Radu for gold mines in S. Africa (Radu *et al*., 1997).

In the most cases we observed the multidimensional character ($d_{min} > 10$) of reconstructed phase spaces of rock cracking and the destruction processes on different scales for the **energy** distribution. Three kinds of phase spaces with a growing number of dimensions were distinguished: (A) spaces with dimension ≤10, (B) spaces with dimensions within the range of 11–15 and (C) spaces with undefined dimensions >15 and >>15. Spaces of type (A) characterised seismic processes referring to *AE* of syenite and sandstone in the "after destruction" stage (T13b/c) and Volcanism 1, type (B)

was connected with *AE* of granite in stages (a) and (b), coal mining in the *Wujek* and *AE* of P3b and S4c. Type (C) was connected to the rest of processes (exploitation of coal in *Katowice*, copper and gold mines, as well as Volcanism 2 and the activity of the San Andreas fault). The obtained dimensions of attractors indicate the presence of chaotic behaviour of higher order for all kinds of seismicity induced by the *Wujek* mine as well as the activities of Yake-dake in the first period of recording. Chaos of lower order manifests itself in energy distribution of *AE* of all three examined samples (P3c, T13b/c, S4a and S4b). The determination of the dimensions of attractors in other systems was impossible, although the curves $D_2(d)$ in some of them (distinct change of curve inclination) suggested the possibility of saturation for $d > 15$. Such a classification does not fit the curves for Volcanism 2 and N. California, the growth of which in the whole of range d is almost linear and no major changes in the curve inclination were observed.

In the case of **time** distribution of seismic events, the dimensions of reconstructed phase spaces in most (8/10) cases group between $d_{min} = 3$ and 5. Such a number of independent variables describing tremor making processes was observed for the data referring to natural seismicity (except Etna) starting from 3–4 variables for the activities of Yake-dake volcano and the San Andreas fault in both parts of California through 4 independent variables for copper mining in Legnica-Głogów District to 5 variables for coal mining in Upper Silesia. The low dimension of reconstructed phase spaces suggests a possibility of predicting the evolution of these systems. The second type of reconstructed phase spaces consists of spaces of dimensions 8-10. This included spaces obtained for time distribution of seismic events induced by coal mining in the *Wujek* mine and gold mining in S. Africa. The dimension of phase space reconstructed based on the temporal sequence of "time" in the case of copper mining has the same value (4) as for Volcanism 2 and N. California data. The compliance of the attractor dimension D_2 was also obtained here. For time distribution, D_2 of the attractor in all cases is equal to 1.0–1.12. Slightly larger values were observed for data from: N. California, Sicily, *Katowice* ($D_2 = 1.16$–1.18.) and S. Africa (1.3).

For the **surface and space** distribution of the tremor sources, the same three kinds of reconstructed phase spaces as for energy distribution were distinguished. In most cases (6/7) the inclusion in the given group for epicentres distribution agrees with the membership in the same group for the hypocenters. The first group includes spaces of dimensions ≤10. Reconstructed spaces for data concerning natural seismicity of Volcanism 2 in Japan and the San Andreas fault in S. California belong to this category. For *xyz* distribution also the data from the area of Etna are within this group. The analysis shows that these processes are ruled by deterministic chaos of lower order. A relatively low dimension of these spaces gives the opportunity to forecast the time evolution of the systems for which they were reconstructed. The second group includes phase spaces of seismic processes induced by coal mining (*Wujek* and *Katowice*) and tremors connected with Volcanism 1. Seismic processes in these two

mines differ significantly in the dimension of the attractor: 5.74 and 7.92, respectively. This can indicate a different degree of determinism in these systems. In the case of Volcanism 1, the dimension of the attractor is 5.34. Dimensions D_2 of the attractors indicate the presence of chaotic phenomena of the higher order. Generally, for hypocenters distribution, chaos of the lowest order was discovered in the volcanism of Etna and Yake-dake in the second phase of tremors (the same dimension of the attractor) and seismicity of the San Andreas fault in the southern part of the region, chaos of the higher order – in the Yake-dake in the first phase of tremors, and that of the highest order – in the *Katowice* mine. For data from the gold mine in S. Africa and N. California the determination of D_2 was impossible because of the lack of stabilisation level.

The calculation of the sign of maximum **Lyapunov's exponent** was intended to definitely confirm the presence or lack of chaotic behaviour ($\lambda_{max} > 0$ or < 0) in the evolution of individually examined systems. The following remarks and conclusions have been drawn:

– The estimation of the largest positive Lyapunov's exponent for the examined data sets in 48% cases produced positive values confirming the presence of deterministic chaos in different-scale processes of rock cracking. The presence of chaotic behaviour was primarily detected in the time distributions of tremors (90%) and coordinates of tremor sources (57% for *xyz*) mainly for natural seismic activity.

– The values of the largest Lyapunov's exponent ranging between negative and positive values make up 21% of the obtained results and they are ambiguous and difficult to interpret.

– In 13 cases (31%) the exponent was negative, which means that in those systems deterministic chaos was not detected. Such a result referred especially to the distributions of energy of tremors (53%) and epicentres (30%). The negative Lyapunov's exponent can result from a small length of analysed data sets (e.g., *Wujek*) or energy cuts. Such a result concerned energy distributions for all the data sets referring to natural seismic activity, some sets referring to mining-induced seismic activity *(Polkowice-Sieroszowice*, *Wujek*, the gold mine in S. Africa) and *AE* of granite sample in the "after destruction" phase .

The compliance of the results of the largest Lyapunov's exponent was observed for the following distributions: energy, time, surface and space for different types of seismic activity with the results of the studies on phase space of these phenomena. Particularly convincing were the results obtained for all the examined distributions of seismic activity for *Polkowice-Sieroszowice*, Etna, Volcanism 2 and S. California. The positive sign of λ_{max} corresponded to the phase spaces group (A) and low dimension of the attractor (< 4.32). This confirmed the presence of deterministic chaos in seismic activities of these systems. A negative sign, suggesting the lack of chaotic behaviour coincided with the classification of the examined processes into groups (B) or (C) and

the high dimensional attractor. Similar compliance was obtained for the distribution of the intensity of energy emitted during the test of compressing a granite sample S4 (all phases) and, except for energy distribution, also for Volcanism 1 (a total of 48% cases). Partial confirmation of the compliance in the analysis of phase space and λ_{max} was observed for time distribution in *Rudna*, S. Africa, *Katowice* and N. California. The results confirmed the presence of chaos in the systems. The compliance of both analyses eliminated the possibility of chaotic behaviour in the case of energy distribution in S. Africa and N. California and for coordinates *xy* and *xyz* of Volcanism 1. The results obtained for *xy* and *xyz* in *Katowice*, and *xyz* for *Wujek* as well as *AE* for samples P3c and T13b/c are unclear. These systems were characterised by $d_{min} = 7–14$, $D_2 = 3.41–7.92$ and the sign of λ_{max} ranged between positive and negative (12% cases). Such results indicate a certain probability of the presence of chaotic behaviour in the systems. In the remaining cases (26%), the results of the analysis of the largest Lyapunov's exponent did not correspond to those of the phase space or were contradictory to them. One could not answer whether chaos was present in those systems or not.

6. OVERALL CONCLUSIONS

– Generally speaking, in all the data sets examined as to the presence of non-linear dynamics, the multifractality of analysed seismic parameters and symptoms of deterministic chaos were observed.

– The comparison of the obtained results confirmed the universality of the selected parameters of chaotic dynamics referring to different scales of the processes of rock fracturing and destruction as well as the usefulness of the applied methods of data analysis for the qualitative description of seismic processes.

– Based on the analysis of the generalised dimension spectrum, certain qualitative differentiation of the studied groups of seismic processes of a different scale can be provided. Natural seismicity turned out to be a more heterogeneous and lower-dimension process compared to induced seismicity, while the most homogeneous distributions and the highest dimensions D_∞ were obtained for seismo-acoustic emissions. The most important exceptions included: *Polkowice-Sieroszowice*, *Katowice* and the syenite sample P3c. For them, the degree of heterogeneity and the value of the estimate of generalised dimension in some distributions were close to the ones obtained for natural seismicity. On the other hand, low heterogeneity and large values of the dimension for the time distribution were obtained for Etna and N. California.

– Reconstructed phase spaces generally turned out to be multi-dimensional. The number of independent variables necessary for the description of the induced seismicity processes was, in some cases, extremely difficult to define and did not produce clear results. This problem could have resulted from different factors: non-stationary

character of the system, short sets of data or 'noise' in the data having a direct influence on the reduction of the linearity interval as a function log$C(R)$ *vs.* log$R$, hence they can lead into the instability of curve $D_2(d_{min})$.

– The obtained dimensions of the attractors of individual fracturing processes were in every case fractal and indicated:

(i) chaos of the lower order for natural seismicity (S. California, Volcanism 2, Sicily) and *AE* of P3c and T13b/c samples, for which the dimension is 3.41–4.29;

(ii) chaotic behaviour of higher order (high-dimension phase space) in the case of induced seismicity (by coal exploitation) and *AE* of S4 sample in stages (a) and (b), because their values concentrate within the range of 4.42–6.89, and for *Katowice* (*xy*) – even reach 7.92;

(iii) the dimension of the attractor reconstructed from the time series of "time", with certain exceptions, also reflect such a classification. For the category of lower order chaos one can include the same systems, except for Sicily, but with Volcanism 1 (dimensions 1.00–1.09); in the category of higher order chaos seismicity induced by mining of coal, copper and gold as well as natural seismicity near Etna and in N. California (1.10–1.30) could be included.

– Finally, based on the largest Lyapunov's exponent, the confirmation of the presence of chaotic behaviour was obtained in seven out of sixteen examined cases. The applied methods of data analysis, despite their confirmed universal character in different scales, do not offer clear solutions, but they indicate the character of the problems and the direction for further research. In future works, the application of a holistic analysis of the sequence of seismic events in phase space might be useful. The dimension of the space would then be defined *a priori* by the number of available parameters characterising a set of events. All the seismic parameters available for a given set of events would become the coordinates of the space and they would be analysed simultaneously. In such a space, the system attractor would be reconstructed.

References

Baker, G.L., and J.P. Gollub, 1995, *Chaotic Dynamics – an Introduction*, Cambridge University Press, Cambridge, 192 pp.

De Luca, L., S. Lasocki, D. Luizio and V. Massimo, 1999, *Fractal dimension confidence interval estimation of epicentral distributions*, Ann. Geof. **42**, 5, 911-25.

Eneva, M., 1996, *Effect of limited data sets in evaluating the scaling properties of spatially distributed data: an example from mining-induced seismic activity*, Geophys. J. Int. **124**, 773-786.

Grassberger, P., and I. Procaccia, 1983, *Measuring the Strangeness of Strange Attractors*, Physica **9 D**; Nonlin. Phenomena, North-Holland Publ. Comp., Amsterdam, 189-208.

Idziak, A., and W.M. Zuberek, 1995, *Fractal analysis of mining induced seismicity in the Upper Silesian Coal Basin*. **In:** H.-P. Rossmanith (ed.), Proc. Int. Conf. "Mechanic of Jointed and Faulted Rock", Vienna 1995, Balkema, Rotterdam, 679-682.

Laskownicka, A., 1999, *The potential forecasting abilities of selected parameters of the seismic tremors series: examples from coal, copper and gold mines*, Publs. Inst. Geophys. Pol. Acad. Sc. **M-22** (310), 257-265 (in Polish with English abstract, table and figure captions).

Lasocki, S., and B. Kustowski, 2002, *Analysis of deflection for identification of epicenter migration directions of swarm activity from Hida Mountains in Japan*, Acta Geophys. Pol. **50**, 1-12.

Lasocki, S., and Z. Mortimer, 1998, *Variations of MS source distribution geometry before a strong tremor occurrence in mines.* **In:** H.R. Hardy (Jr.), Proc. of the 6th Conference on "Acoustic Emission/Microseismic Activity in Geologic Structures and Materials", Trans. Tech. Publs., Clausthal, 325-337.

Majewska, Z., and Z. Mortimer, 1998, *Fractal description of acoustic emission produced in systems: coal-gas and coal-water.* **In:** K. Ono (ed.), "Progress in Acoustic Emission IX Transition in AE for the 21th Century, Proc. of Intern. AE Conference", 109-118.

Majewska, Z., and Z. Mortimer, 2000, *Studies of the non-linear dynamics of acoustic emission generated in rocks*, Proc. of 24th European Conference on Acoustic Emission Testing EWGAE, Senlis, France, 1-7.

Majewska, Z., Z. Mortimer and A. Cichy, 2000, *Non-linear dynamics application for the description of accoustic emission phenomena in rocks*, Dokumentacja AGH (unpublished, in Polish).

Mane, R., 1981, *On the dimension of the compact invariant sets of certain non-linear maps in dynamical systems and turbulence*. **In:** D.A. Rand and L.S. Young (eds.), "Dynamical Systems and Turbulance Lecture Notes in Mathematics", Springer-Verlag, Berlin, **898**, 230-242.

Marcak, H., 1995, *Fractal properties of the seismic records sets from mines.* **In:** "Poradnik Geofizyka Górniczego", Biblioteka Szkoły Eksploatacji Podziemnej, Kraków, **2**, 208-213 (in Polish).

Mendecki, A.J., 1997, *Principles of monitoring seismic rockmass response to mining.* **In:** S.J. Gibowicz and S. Lasocki (eds.), "Rockburst and Seismicity in Mines", Balkema, Rotterdam, 69-80.

Mortimer, Z., 1997, *Fractal statistics for the local induced seismicity in some Polish coal mines.* **In:** S.J. Gibowicz and S. Lasocki (eds.), "Rockburst and Seismicity in Mines", Balkema, Rotterdam, 49-53.

Mortimer, Z., 2001a, *Studies on the chaotic dynamics of mining induced seismicity.* **In:** H. Ogasawara, T. Yanagidani and M. Ando (eds.), "Seismogenic Process Monitoring", Balkema, Rotterdam, 341-354.

Mortimer, Z., 2001b, *An analysis of non-linear dynamics of the induced seismicity – fractals and chaos.* **In:** J. Dubiński, Z. Pilecki and W. Zuberek (eds.), "Badania Geofizyczne w Kopalniach", Wyd. IGSMiE PAN, Kraków, 147-151.

Mortimer, Z., and A. Cichy, 2001, *Nonlinear dynamics parameters estimated from the induced seismicity in Polish coal mines*, Acta Geophys. Pol. **49**, 3, 303-316.

Mortimer, Z., and S. Lasocki, 1996, *Studies of fractality of epicentre distribution geometry in mining induced seismicity*, Acta Mont. **A**, 10 (102), 31-37.

Mortimer, Z., Z. Majewska and S. Lasocki, 1999a, *Generalised fractal dimension of induced seismicity and acoustic emission*, Publs. Inst. Geophys. Pol. Acad. Sc. **M-22** (310), 89-94 (in Polish with English abstract, table and figure captions).

Mortimer, Z., A. Marchewka and A. Cichy, 1999b, *The pursuit of deterministic chaos or the study of non-linear dynamics of induced seismicity.* **In:** Materiały V Konferencji Nauk.-Techn. "Geofizyka w Geologii, Górnictwie i Ochronie Środowiska", Kraków, 23 czerwca 1999, 282-289.

Nerenberg, M.A.H., and C. Essex, 1990, *Correlation dimension and systematic geometric effects*, Phys. Rev. **A 42**, 7065-7074.

Packard, N.H., J.P. Crutchfield, J.D. Farmer and R.S. Shaw, 1980, *Geometry from a time series*, Phys. Rev. Lett. **45**, 712-716.

Radu, S., M. Sciocatti and A.J. Mendecki, 1997, *Nonlinear dynamics of seismic flow of rock.* **In:** A.J. Mendecki (ed.), "Seismic Monitoring in Mines", Chapman & Hall, London, 159–177.

Takens, F., 1980, *Detecting strange attractors in turbulence.* **In:** D.A. Rand and L.S. Young (eds.), "Dynamical Systems and Turbulence", Lecture Notes in Mathematics, Springer-Verlag, Berlin, **898**, 366-381.

Wolf, A., J.B. Swift, H.L. Swinney and J.A. Vastano, 1985, *Determining Lyapunov exponents from a time series*, Physica **16D**, 285-317.

Received 11 August 2003
Accepted in revised form 10 March 2004